

2013


## Article Navigation Wild-type Measles Virus Infection Upregulates Poliovirus Receptor-Related 4 and Causes Apoptosis in Brain Endothelial Cells by Induction of Tumor Necrosis Factor-Related Apoptosis-Inducing Ligand

Haniah Abdullah  
*Queens University Belfast*

Brenda B. Brankin  
*Technological University Dublin, [brenda.brankin@tudublin.ie](mailto:brenda.brankin@tudublin.ie)*

Clare Brady  
*Queens University Belfast*

Follow this and additional works at: <https://arrow.tudublin.ie/scschbioart>  
See next page for additional authors

 Part of the [Biology Commons](#)

### Recommended Citation

Abdullah, H., Brankin, B., Brady, C. & Cosby, S. (2013). Wild-type measles virus infection upregulates poliovirus receptor-related 4 and causes apoptosis in brain endothelial cells by induction of tumor necrosis factor-related apoptosis-inducing ligand. *Journal of Neuropathology & Experimental Neurology*, 72 (7), pp. 681–696, doi:10.1097/NEN.0b013e31829a26b6

This Article is brought to you for free and open access by the School of Biological Sciences at ARROW@TU Dublin. It has been accepted for inclusion in Articles by an authorized administrator of ARROW@TU Dublin. For more information, please contact [arrow.admin@tudublin.ie](mailto:arrow.admin@tudublin.ie), [aisling.coyne@tudublin.ie](mailto:aisling.coyne@tudublin.ie).



This work is licensed under a [Creative Commons Attribution-Noncommercial-Share Alike 4.0 License](#)

---

**Authors**

Haniah Abdullah, Brenda B. Brankin, Clare Brady, and Sara Louise Cosby

ORIGINAL ARTICLE

# Wild-type Measles Virus Infection Upregulates Poliovirus Receptor–Related 4 and Causes Apoptosis in Brain Endothelial Cells by Induction of Tumor Necrosis Factor–Related Apoptosis-Inducing Ligand

Hani'ah Abdullah, PhD, Brenda Brankin, PhD, Clare Brady, BSc,  
and Sara Louise Cosby, PhD, FRCPath, FSB

## Abstract

Small numbers of brain endothelial cells (BECs) are infected in children with neurologic complications of measles virus (MV) infection. This may provide a mechanism for virus entry into the central nervous system, but the mechanisms are unclear. Both in vitro culture systems and animal models are required to elucidate events in the endothelium. We compared the ability of wild-type (WT), vaccine, and rodent-adapted MV strains to infect, replicate, and induce apoptosis in human and murine brain endothelial cells (HBECs and MBECs, respectively). Mice also were infected intracerebrally. All MV stains productively infected HBECs and induced the MV receptor PVRL4. Efficient WT MV production also occurred in MBECs. Extensive monolayer destruction associated with activated caspase 3 staining was observed in HBECs and MBECs, most markedly with WT MV. Tumor necrosis factor–related apoptosis-inducing ligand (TRAIL), but not Fas ligand, was induced by MV infection. Treatment of MBECs with supernatants from MV-infected MBEC cultures with an anti-TRAIL antibody blocked caspase 3 expression and monolayer destruction. TRAIL was also expressed in the endothelium and other cell types in infected murine brains. This is the first demonstration that infection of low numbers of BECs with WT MV allows efficient virus production, induction of TRAIL, and subsequent widespread apoptosis.

**Key Words:** Apoptosis, Brain endothelial cells, CNS, Measles virus, PVRL4, Subacute sclerosing panencephalitis (SSPE), TRAIL.

From the Centre for Infection and Immunity (HA, CB, SLC), School of Medicine Dentistry and Biomedical Sciences, Queen's University Belfast, UK; and School of Biological Sciences (BB), Dublin Institute of Technology, Dublin, Ireland.

Send correspondence and reprint requests to: Sara Louise Cosby, PhD, FRCPath, FSB, Queen's University Belfast, School of Medicine, Dentistry and Biomedical Sciences, Centre for Infection and Immunity, 4th Floor, Medical Biology Centre, Lisburn Rd, Belfast BT9 7BL UK; E-mail: l.cosby@qub.ac.uk

This work was performed with financial support from the Health and Personnel Social Services for Northern Ireland R&D Office (Grant No. 9.1) and the Queen's University of Belfast.

## INTRODUCTION

In systemic measles virus (MV) infection, lesions are centered on small venules, but virus has not been detected in brain parenchyma in healthy individuals without neurologic complications or in postinfection MV encephalomyelitis (1). However, Esolen et al (2) found MV RNA in the brain endothelial cells (BECs) of children who died with severe acute measles encephalitis 3 to 10 days after the onset of a rash. Measles virus infection in children who are immunocompromised frequently results in virus infection of neural tissue, most likely as a result of damage to the blood-brain barrier (BBB), with subsequent development of measles inclusion body encephalitis (MIBE) (3, 4). We previously found that a small number of cells in the cerebral endothelium of some blood vessels are infected in the long-term MV complication subacute sclerosing panencephalitis (SSPE) (5). In both diseases, BEC infection is likely to play a major role in viral spread into surrounding brain tissue, which is facilitated by damage to the BBB by virus-induced apoptosis.

Transport of MV into the brain in virus-infected leukocytes has been suggested as an alternative mechanism to direct infection of BECs. Both mechanisms likely occur, but to different extents, and both have been demonstrated in an experimental canine distemper virus model (6). Dittmar et al (7) showed that transendothelial cell migration of infected T cells is strongly inhibited, but virus was transferred from T cells to polarized human BECs (HBECs) with subsequent release from both apical and bipolar surfaces. Therefore, the latter may be the major mechanism involved in MV entry into the central nervous system (CNS) parenchyma.

Although HBEC cultures may closely reflect infection of the human cerebral endothelium, small animal models are required to understand how MV spreads from infected endothelium to other cell types in the CNS as well as the associated immune response. We have previously shown that, unlike the rodent-adapted strain, which causes acute encephalitis, wild-type (WT) MV causes a persistent infection without clinical signs. Using both in vitro and ex vivo infection models, we showed that WT MV infected neurons and oligodendrocytes and, to a lesser extent, astrocytes in the murine CNS (8). Therefore, this model reflects the situation in the early stages of SSPE and

MIBE. However, infection of the murine endothelium in this model was not examined.

We previously reported that the Hu2 vaccine strain of MV can infect murine brain endothelial cells (MBECs) in vitro and enhance adhesion of leukocytes to these cells in a manner similar to what occurs in HBECs (9, 10). Human BECs in vivo show a high level of expression of the cell entry receptor for vaccine strains of MV, CD46 (11, 12), and these cells can be infected in vitro to a high level by MV vaccine strains, probably because of their high affinity for this molecule. The percentage of infected HBECs with WT MV strains is generally considerably lower (13), probably because these viruses do not use CD46 as a receptor and endothelial cells (ECs) do not express signaling lymphocyte activation molecule (SLAM), the cell receptor used by WT viruses on immune cells (14, 15). Murine BECs, like other murine cells, do not express forms of SLAM or CD46. Therefore, cell entry by WT virus in HBEC and all MV strains in MBEC is both CD46 and SLAM independent. It is not known if BECs express the newly recognized receptor for WT MV (on polarized epithelial cells), polio receptor-related 4 (PVRL 4), also known as Nectin-4 (16, 17).

In contrast to other WT MV stains examined, the WT Wü4797 strain has been reported to give higher infection levels in HBECs. It remains unclear as to why certain WT strains spread better in these cells than others (13). In view of this, we investigated WT MV infection in these cells. Furthermore, if WT MV infection in HBECs and MBECs show similar characteristics, this would validate the use of a murine in vivo model for the study of infection at the BBB.

Here, our aim was to establish parallel in vitro and in vivo murine model systems of WT MV infection to reflect the human diseases SSPE and MIBE and to use these systems to examine the mechanism of BEC damage and subsequent virus spread. This may also be relevant to other viral infections that gain entry to the CNS through the BBB. We compared infection of a strain of WT MV, Dublin 3267 (not previously used to infect BEC),

with vaccine and rodent-adapted viruses in both HBECs and MBECs. We also examined the mechanism of apoptosis in these cell lines as well as in the infected murine CNS.

## MATERIALS AND METHODS

### Cell and Virus Stocks

Human BECs were obtained from 3H Biomedical (Uppsala, Sweden) and grown in EC medium with EC growth supplement (containing 5% fetal calf serum, 1% penicillin/streptomycin, and EC growth supplement) from the same company. The isolation and characterization of primary cultures of MBECs from mice were carried out as previously described (9). Briefly, EC cells were sorted by fluorescence-activated cell sorting (FACS-IV; Becton-Dickinson, Mountain View, CA) using the plant lectin *Griffonia (Bandiera) simplicifolia IB4* (GSA-I), which is specific for murine EC in vitro and in vivo. Astrocyte contamination was ruled out by using anti-gial fibrillary acidic protein antibody (Ab) (Dako, Carpinteria, CA). In addition, confluent monolayers of MBECs were stained before use for *Ulex europaeus* agglutinin I, a specific marker that distinguishes ECs from other cell types including astrocytes and pericytes. Murine BEC preparations used in these experiments were routinely 95% to 99% pure and used between passages 6 and 12. CHO-PVRL4 cells were a kind gift from Dr. Christopher Richardson (Dalhousie University, Halifax, Canada). MBEC and Vero/Vero human SLAM (VeroHSLAM) cells were passaged and maintained in high-glucose DMEM supplied with 20% or 10% heat-inactivated fetal bovine serum (Gibco, Carlsbad, CA), respectively, and 1% penicillin/streptomycin (PAA; Pasching, AT). CHO-PVRL-4 and B95a cells were passaged and maintained as for the other cell lines except F12 medium (Gibco) and RPMI-1640 (Gibco) were used, respectively. VeroHSLAM and CHO-PVRL4 cells require medium containing 400 µg/ml geneticin (Gibco) to retain the SLAM and PVRL4 plasmids respectively. Virus stocks of Edmonston MV vaccine, Schwarz GFP vaccine (a kind gift

**TABLE.** Antibodies Used for Immunofluorescence

Primary Antibodies					
Cell Marker	Detected Structure	Host Species	Dilution	Supplier (Catalog No.)	Reference
Anti-PVRL4	Membrane	Mouse monoclonal	1:100	Abcam, Cambridge, UK (ab57873)	
Anti-PVRL4	Membrane	Rabbit polyclonal	1:100	Abcam (ab155692)	
Anti-CD34	Membrane	Rat monoclonal	1:50	Abcam (ab8158)	(22)
Anti-TRAIL	Membrane	Mouse monoclonal	1:100	Abcam (ab10516)	(23)
Anti-caspase 3	Cleavage site of human caspase 3	Rabbit polyclonal	1:500	Sigma, St. Louis, MO (C8487)	(24)
Anti-measles	Nucleocapsid protein	Mouse monoclonal	1:100	Oxford Biotechnology, Oxford, UK (OBT0055)	(8)
Anti-MAP-2	Microtubules	Mouse monoclonal	1:100	Chemicon/Millipore, (1284959)	(8)
Anti-GFAP	Intermediate filament	Rabbit polyclonal	1:200	DakoCytomation (Z0334)	(8)
Fluorochromes					
Type			Dilution	Supplier (Catalog No.)	Reference
Alexa Fluor 568 goat anti-mouse IgG			1:500	Life Technologies, Grand Island, NY (A-11004)	(25)
Alexa Fluor 568 goat anti-rabbit IgG			1:500	Life Technologies (A-11036)	(26)
Alexa Fluor 488 goat anti-mouse IgG			1:500	Life Technologies (A-11001)	(27)
Alexa Fluor 488 goat anti-rabbit IgG			1:500	Life Technologies (A-11008)	(28)
Alexa Fluor 568 goat anti-rat IgG			1:200	Life Technologies (A-11077)	(29)

TRAIL, tumor necrosis factor-related apoptosis-inducing ligand.

from Prof. Frederick Tangy, Pasteur Institute, Paris, France) (18) and CAM/RB rodent-adapted MV (19) were grown in Vero cells. The WT MV strain, Dublin-3267 (20), was grown and titered in B95a cells. All experimental infections and treatments were carried out at least in triplicate.

### Mouse Infections

Two- to three-day-old C57BL6 mice were obtained from in-house breeding colonies in the Biological Research Unit, Queen's University Belfast and were used in animal experimentation under approved university regulations and a UK Home Office License. Mice were killed by lethal injection of anesthetic (pentobarbital euthanasia). At least 3 mice were inoculated intracerebrally with  $10^4$  TCID<sub>50</sub> of each virus in 25- $\mu$ l volumes. Mouse brains were fixed in 10% formol saline.

### Immunohistochemistry

Whole brain sections (8-mm thick) were cut from 3 levels of paraffin-embedded brain tissue using a microtome. The levels were cut to an approximate depth of 100  $\mu$ m and were separated by 50  $\mu$ m. Formalin-fixed sections were dewaxed and pretreated, as previously described (21). Sections were incubated with monoclonal mouse anti-measles (OBT0055; Oxford Biotechnology, Oxford, UK) diluted 1:2000 followed by the EnVision + system HRP with diaminobenzidine DAB staining (DakoCytomation, Glostrup, Denmark) according to the protocol supplied by the manufacturer and stained with hematoxylin. Sections from normal mouse brain were treated in the same way, and negative control sections were treated with buffer rather than primary Ab.

### Immunocytochemistry/Immunofluorescence

Brain endothelial cells were grown on coverslips and infected or mock infected (with medium). Coverslips cultures were fixed with 4% paraformaldehyde and permeabilized with 0.1% Triton X-100 (Sigma, Dorset, UK) then washed and blocked with 0.5% bovine serum albumin (Sigma). Immunocytochemistry for EC-specific staining was carried out using biotinylated *U. europaeus* agglutinin (Vector Laboratories, Peterborough, UK) diluted 1:500. Primary and secondary antibodies used for immunofluorescence, dilutions, and references are listed in the Table (8, 22–29). Coverslips were mounted in Vectashield mounting medium with DAPI (Vector Laboratories). Activated caspase 3 antigen expression was examined using an APO Active 3 kit according to the manufacturer's instructions (Cell Technology, Mountain View, CA). Staining of mock-infected culture controls was carried out using the secondary Ab either with an isotype control or without primary Ab. Positive cells were counted in 10 fields selected at random in each of 3 cultures. The percentages of positive cells were estimated, and an average was taken for the total number of fields. Images were examined under a confocal laser scanning microscopy (TCS SP5 Leica) or a TE2000-U (Nikon, UK) microscope.

### Ultraviolet Inactivation of Virus

Supernatants isolated from infected or uninfected cultures were centrifuged at 1,000 rpm for 5 minutes to remove cell debris. One-milliliter samples of each supernatant were then placed in 400 mm Petri dishes and ultraviolet (UV)-inactivated at

12.11 J for 10 minutes in a UV cross-linker (Syngene, Cambridge, UK) to inactivate the infectivity of the virus. Samples were tested for infectivity by inoculating VeroHSLAM cell cultures and examining these for a cytopathic effect for 7 days.

### Quantitative Measurement of Tumor Necrosis Factor–Related Apoptosis-Inducing Ligand

The level of soluble tumor necrosis factor–related apoptosis-inducing ligand (TRAIL) in cell supernatants was measured by sandwich enzyme immunoassay ELISA (USCN Life Science, Inc., Wuhan, China), according to the manufacturer's instructions, with a detection range of 0.156 to 10 ng/ml. The optical density was measured in a Mitras LB 940 (Berthold Technology, Bad Wildbad, Germany).

### Soluble TRAIL Treatment

Approximately 80% to 90% confluent MBEC monolayers were treated with soluble mouse TRAIL (Enzo Life Sciences, Exeter, UK) at concentrations of 1, 50, 100, 500, and 1,000 ng/ml for 24 hours.

### Reverse Transcription–Polymerase Chain Reaction

Primers and reverse transcription–polymerase chain reaction (RT-PCR) conditions for Fas and Fas ligand (FasL) were carried out as described by Fleck et al (30) and for TRAIL as described by Fang et al (31). Primers and conditions for B-actin (21) and for full-length PVRL4 (32) have been previously described.

### Anti-TRAIL Treatment of Supernatants

Murine BECs were infected with WT MV at a multiplicity of infection of 5. At 6 days post infection (dpi), the supernatants were collected and UV inactivated and aliquots were treated with mouse monoclonal anti-TRAIL Ab (Abcam) at concentrations of 5, 10, and 20  $\mu$ g/ml before adding to the MBECs. Controls of no Ab or treatment with 20  $\mu$ g/ml of a non-immune mouse IgG1 isotype (X0931; Dako) were used.

### Statistical Analysis

Statistical analysis was carried out using the *t*-test and the Mann-Whitney U test. Values of  $p < 0.05$  were considered significant (\*),  $p < 0.01$  very significant (\*\*), and  $p < 0.001$  highly significant (\*\*\*).

## RESULTS

### HBECs and MBECs Are Susceptible to All MV Strains

Human BECs were characterized by the supplier. In addition to full characterization at the time of isolation (9), confluent monolayers of MBECs were stained before use for *U. europaeus* agglutinin I; 100% of the cells were shown to be positive (Fig. 1A). Both MBECs and HBECs were infected with Edmonston, CAM/RB, or WT virus at a multiplicity of infection of 5 for 24, 48, and 72 hours and were stained for MV. Syncytia formation was not detected in MBECs infected with these 3 viruses, whereas both Edmonston and the CAM/RB virus induced extensive infection in HBECs with syncytia formation. Wild-type MV antigen was distributed throughout

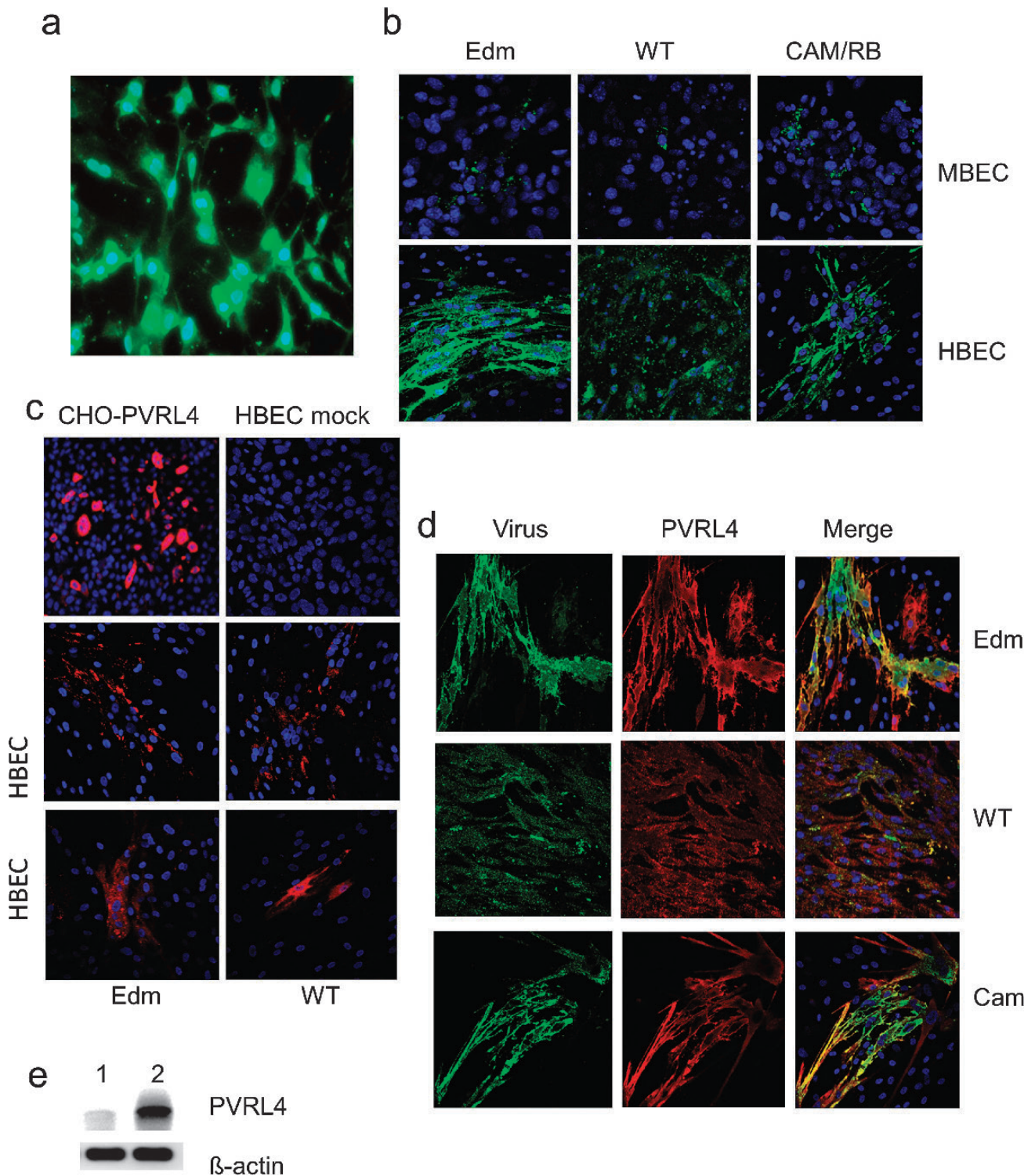


**FIGURE 1.** Wild-type (WT) measles virus (MV) infects brain endothelial cells (BECs) with induction of PVRL4 in human BECs (HBECs). **(A)** Immunocytochemistry for *Ulex europaeus* agglutinin in uninfected murine BECs (MBECs). **(B-D)** MBECs and HBECs were infected at a multiplicity of infection (MOI) of 5 with CAM/RB, Edmonston, and WT MV strains and immunofluorescence staining was carried out. Measles virus (green), PVRL4 (red), and staining of cell nuclei with DAPI (blue) at 72 hours post infection. **(B)** MBECs and HBECs stained for virus. **(C)** HBECs stained for PVRL4; first and second panels show polyclonal antibody (Ab); third panel shows monoclonal Ab. **(D)** HBECs double stained for MV and PVRL-4. **(E)** RNA was extracted from mock infected and WT MV-infected HBEC and RT-PCR carried out for PVRL4 and  $\beta$  actin. Lane 1, mock infected; lane 2, infected. Magnifications: **(A)** 200 $\times$ ; **(B)** MBEC 400 $\times$ , HBEC 200 $\times$ ; **(D)** 200 $\times$ .

the monolayer, but the fluorescence was less intense, reflecting lower levels in cells compared to infection with CAM/RB or Edmonston. Although there was no syncytia formation, cells began to round up and the monolayer disintegrated (Fig. 1B).

In MBECs, approximately 2% of cells showed staining for both WT and CAM/RB at 72 hours post infection (hpi). Edmonston infection showed a significantly lower percentage of antigen-positive cells (Fig. 2A). Wild-type and CAM/RB infection was also compared in HBEC. At 48 hpi, 40% of cells were positive for WT viral antigen. This increased to nearly 60% by 72 hpi. At this time point, 80% of cells were positive in CAM/RB MV cultures (Fig. 2B). Virus titers were measured by TCID<sub>50</sub>. Less than 1 log of infectious virus was detected in Edmonston or CAM/RB virus-infected MBECs up to 72 hpi

(data not shown). The titer of WT MV increased over time, reaching a mean of 10<sup>3.1</sup> TCID<sub>50</sub>/ml at 48 hpi (Fig. 2C). Because both the Edmonston vaccine strain and the vaccine-derived rodent adapted CAM/RB strain show extensive infection in HBECs (probably due to the use of the CD46 receptor), only titers of WT MV were examined in these cells. Titers reached a level similar to those in MBEC of approximately 10<sup>3.5</sup> TCID<sub>50</sub> by 72 hpi (Fig. 2D).

To determine whether PVRL 4 is expressed on HBEC and/or MBEC and could therefore be potentially used as a virus receptor for WT MV, we carried out immunofluorescence staining for PVRL4 on uninfected cells as well as on cells infected with each MV strain at 72 hpi. CHO-PVRL4 cells were used as a positive control. There was no staining for PVRL4 on uninfected

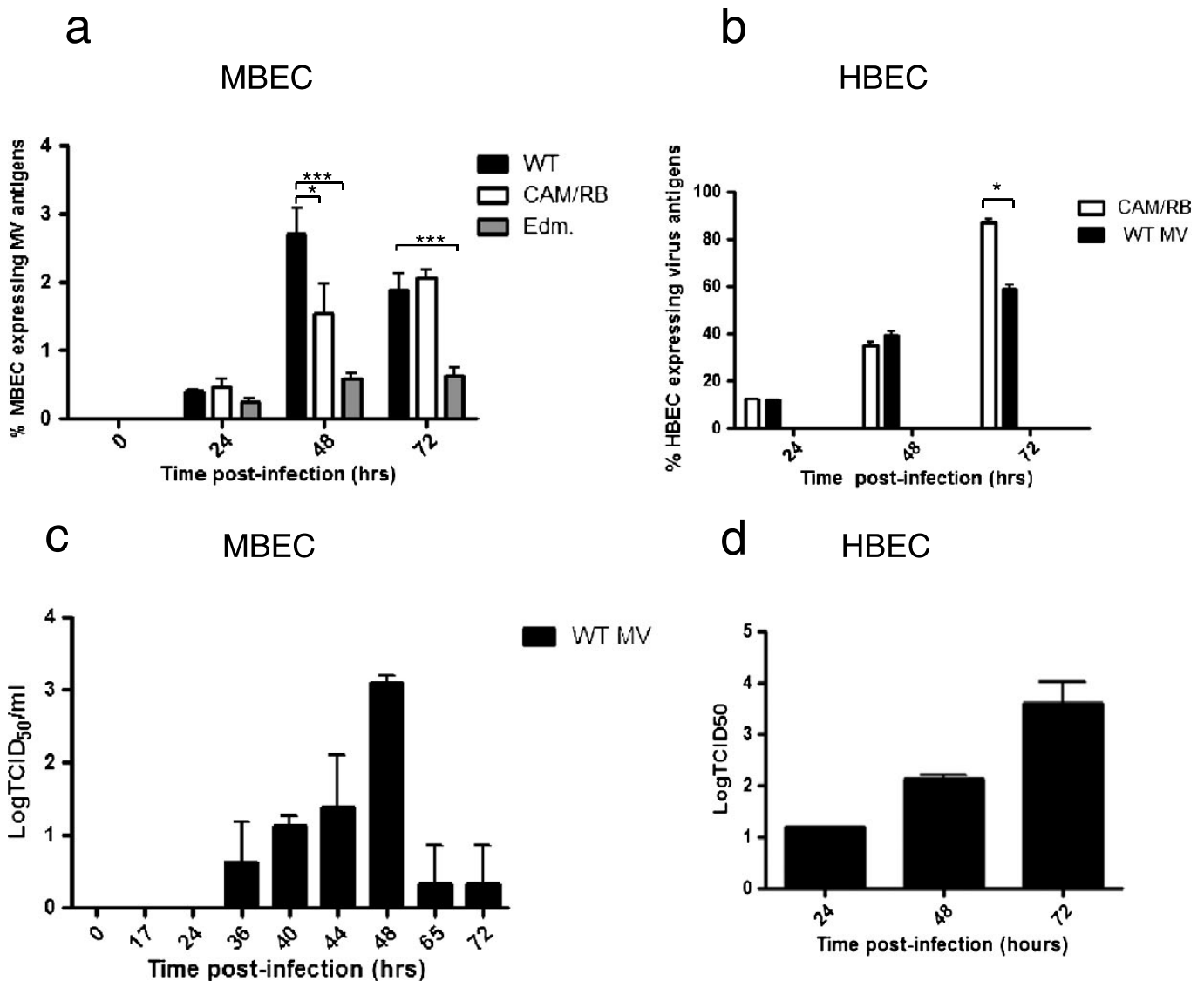


**FIGURE 2.** Efficient production of wild-type (WT) measles virus (MV) by a low percentage of virus antigen-positive murine brain endothelial cells (MBECs). MBECs and human BECs (HBECs) were infected at a multiplicity of infection (MOI) of 5 with CAM/RB, Edmonston, and WT MV strains; MV antigen detection was carried out by immunofluorescence. (A, B) Ten or more fields in each of 3 infected cultures were counted at 24, 48, and 72 hours post infection (hpi) to determine the percentage of MV antigen-positive cells; MBEC (A) and HBEC (B). (C, D) Total virus samples were collected from WT-infected cultures up to 72 hpi. TCID<sub>50</sub> titrations were performed in Vero human SLAM (VeroHSLAM) cells; MBEC (C) and HBEC (D); mean and SD from 3 separate experiments are shown.

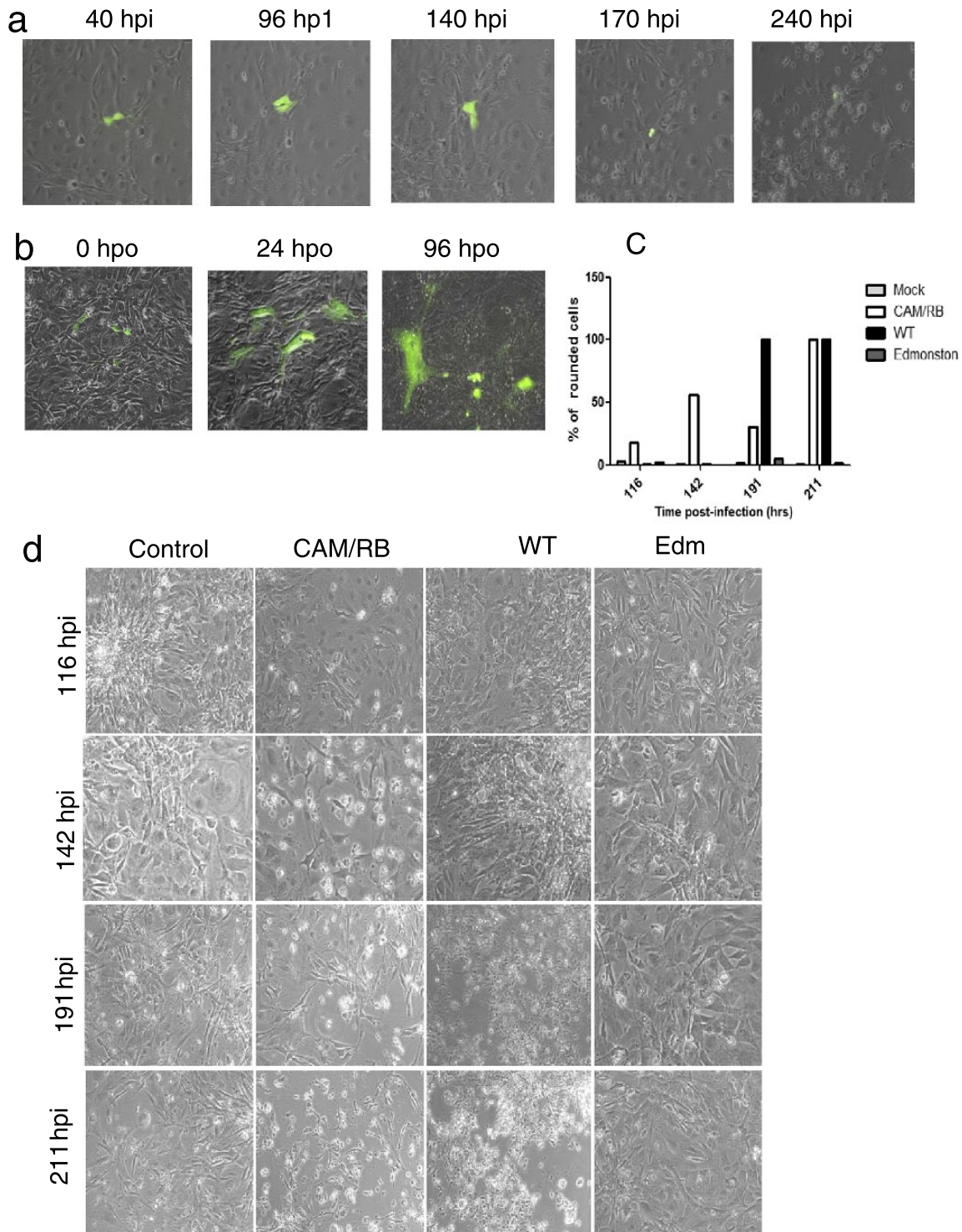


**FIGURE 3.** Extensive apoptosis occurs in noninfected cells in wild-type (WT) measles virus (MV)-infected cultures. **(A)** Murine brain endothelial cells (MBECs) were infected with the Schwarz-GFP vaccine virus at a multiplicity of infection (MOI) of 1. Spread of MV infection in MBEC was monitored over time by examining the same field at 40, 93, 140, 170, and 240 hours post infection (hpi). **(B)** Infected cells were overlaid with Vero cells (permissive for vaccine strains of MV) at 72 hpi. The spread of green fluorescent protein (GFP) was monitored at 24 and 96 hours post overlay (hpo). UV and phase-contrast microscopy images are combined with UV microscopy. **(C, D)** MBEC monolayers were infected with CAM/RB, WT, and Edmonston virus strains at an MOI of 5 and monitored up to 211 hpi. **(C)** The percentage of rounded cells in monolayers was determined by counting 10 fields in each of 3 cultures. **(D)** Dark field microscopy of representative monolayers demonstrates apoptosis in CAM/RB- and WT-infected cultures. Magnification: 200 $\times$ .



HBECs, but surprisingly, localized areas of staining occurred in cells infected with all strains of MV when either single (Fig. 1C) or double staining for MV and PVRL4 (Fig. 1D) was performed. This was demonstrated with both polyclonal and monoclonal antibodies to PVRL4 (Fig. 1C) and was shown to be specific as cultures treated with isotype control antibodies were negative (not shown). No staining for PVRL4 using the cross-reactive polyclonal Ab was seen in either infected or uninfected MBEC (not shown). Reverse transcription-PCR was carried out on RNA extracted from both infected and mock-infected HBECs. A PCR product was obtained in infected cells, but only a very weak band in mock-infected cultures (Fig. 1E).

### Extensive Apoptosis Occurs in Noninfected Cells in WT MV-Infected MBEC Cultures

To determine whether MBEC underwent destruction at a later time than in HBEC cultures, MBECs infected with the 3 virus strains were examined for a prolonged period. In addition, the Schwarz MV vaccine strain, which expresses green fluorescent protein (GFP), also produced negligible amounts of infectious virus (not shown) and was used to follow infection in real time. Schwarz GFP virus remained localized with infectious foci, disappearing by 240 hpi (Fig. 3A). However, when MBECs were overlaid with Vero cells at 24 hpi, virus spread to the latter; infection spread with production of syncytia, which increased in size by 96 hours post overlay (hpo) (Fig. 3B). Between 116 and 211 hpi, there was rounding of cells in monolayers infected with CAM/RB. Cell rounding with WT virus was not observed until 191 hpi but reached similar levels to CAM/RB at 211 hours. Similar extents of cell rounding occurred with the Edmonston vaccine strain compared to mock-infected cultures. The percentage of rounded cells in monolayers was determined by counting 10 fields in each of 3 cultures (Fig. 3C). Representative monolayers are shown in Figure 3D.

To determine whether cell death was caused by apoptosis, immunofluorescence staining for activated caspase 3 was carried out in WT-infected MBECs at 144 hpi. 50.8% ± 7.4% (SE) of the cells were caspase 3 positive compared to less than 1% of cells in mock-infected cultures (Fig. 4A). We compared caspase 3 staining in HBECs infected with the 3 MV strains at 72 hpi. Double staining for virus and caspase 3 showed colocalization, but nearby virus-negative cells were also caspase 3 positive. Caspase 3 staining was widely distributed in the monolayer in WT-infected monolayers, which had low levels of viral antigen throughout. Caspase 3 staining in cultures infected with the other 2 viruses was localized in foci of virus infection (Fig. 4B). Mock-infected cells were caspase 3 negative (not shown).

### Virus-Induced Soluble Factors Cause Apoptosis in MBEC Monolayers

The results suggested that a soluble factor in infected BEC cultures may be responsible for cell rounding and death. This was further investigated by collecting the supernatants from infected MBEC cultures at time points from 24 to 216 hpi and UV radiating them to inactivate the virus. The inactivated supernatants (which were not frozen) were added to fresh monolayers of MBEC and the cultures monitored up to 216 hours. Control supernatants were prepared from mock-

infected cells at the same time points. UV-inactivated supernatants removed from all virus-infected cultures earlier than 96 hpi resulted in no or very minimal effects on fresh cells. Supernatants removed from CAM/RB, WT, and Schwarz-GFP virus-infected cultures at 96 hpi caused cell rounding on fresh monolayers of MBEC between 144 and 216 hours post treatment (hpt). Supernatants removed from WT-infected cultures at 216 hours produced 30.75% ± 4.38% (SE) rounded cells at 144 hpt; supernatants removed at 216 hpi caused total destruction of MBEC monolayers with loss of all cells by 216 hpt. Supernatants isolated from cultures infected with Edmonston virus at 216 hpi showed similar levels of cell rounding (29.7% ± 3.74%) at 144 hpt, and this increased to 39.5% ± 5.12% at 216 hpt. Representative results for WT and Edmonston MV strains are shown in Figure 5A and B, respectively.

To determine whether the factor in the UV-inactivated supernatants was causing apoptosis, we examined monolayers

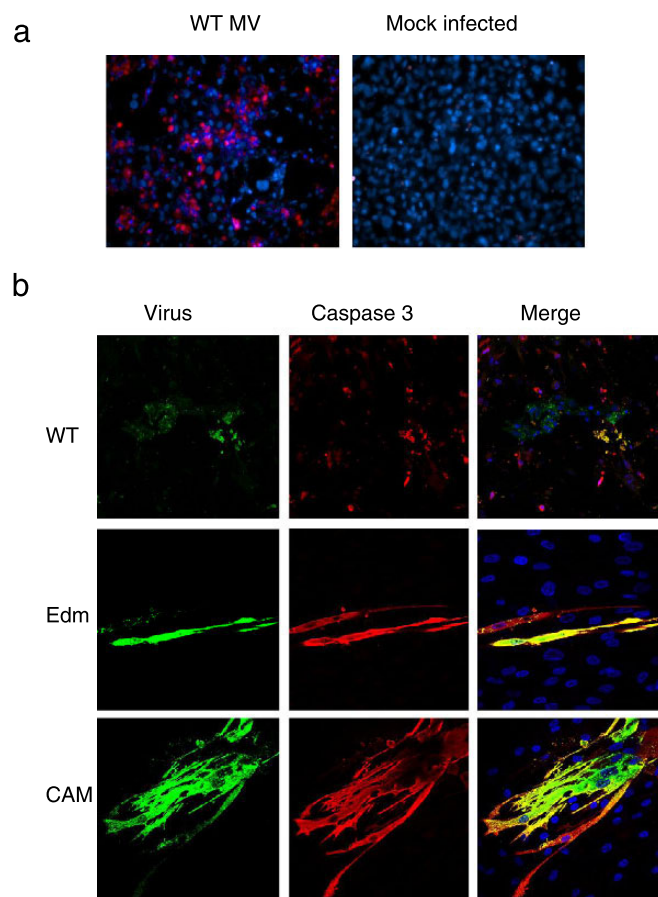


**FIGURE 4.** Activated caspase 3 is expressed in virus-infected cultures. Human brain endothelial cell (HBEC) monolayers were infected with CAM/RB, wild-type (WT), and Edmonston virus measles virus (MV) strains and murine brain endothelial cells (MBECs) with WT MV at a multiplicity of infection (MOI) of 5. Immunofluorescence staining was carried out in infected and mock-infected cultures. **(A)** MBECs at 144 hours post infection (hpi) stained for activated caspase 3 (red). **(B)** HBECs at 72 hpi double stained for virus (green) and caspase 3 (red). Nuclei are stained with DAPI (blue). Magnifications: **(A)** 200×; **(B)** 400×.

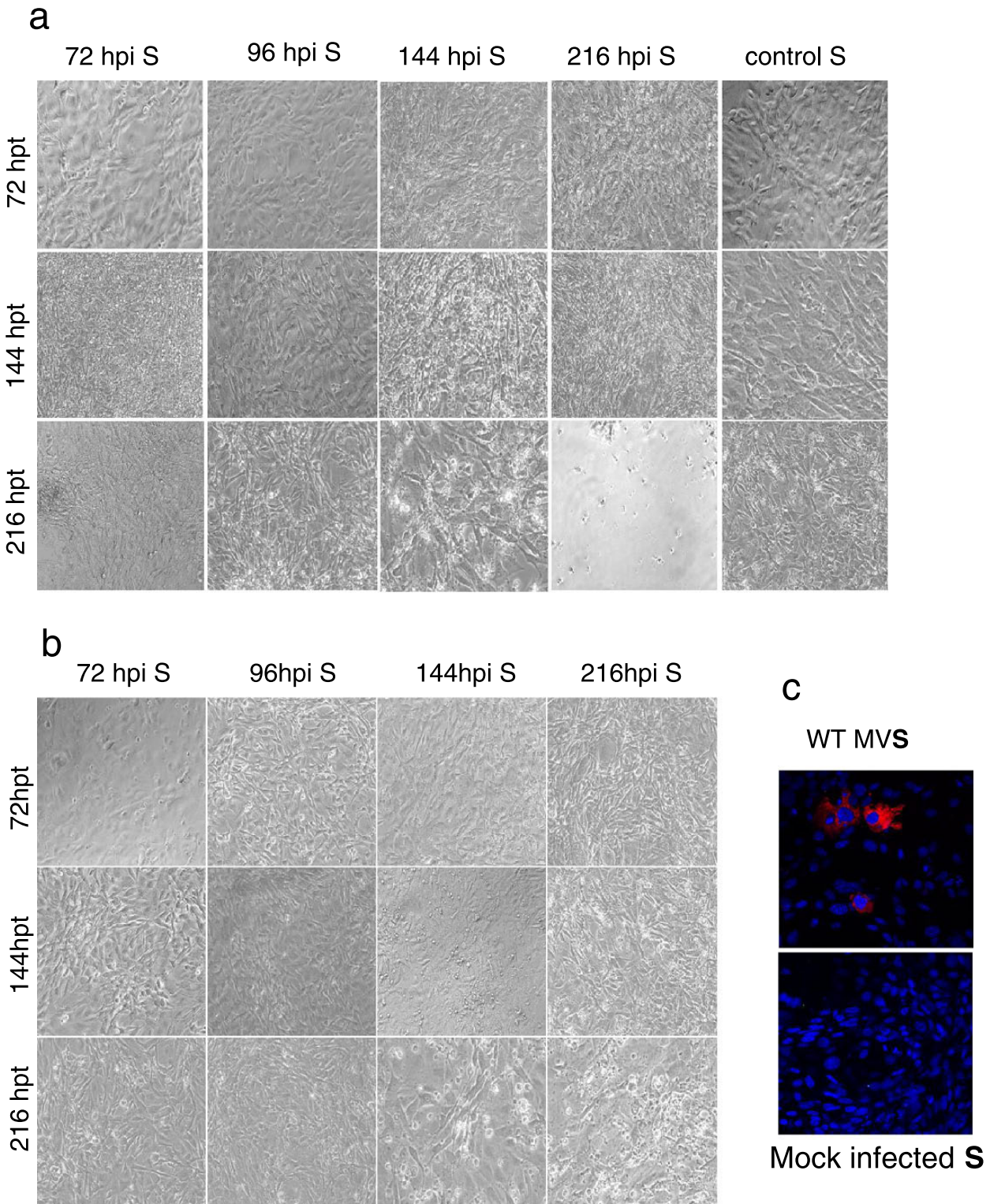


**FIGURE 5.** Virus-induced soluble factors cause apoptosis in monolayers of murine brain endothelial cells (MBECs). Supernatants (S) were collected from MBEC monolayers infected with the wild-type (WT) and Edmonston strains of measles virus (MV) at 72, 96, 144, and 216 hours post infection (hpi) as well as from mock-infected cultures at the same time points. These were UV inactivated and added to fresh MBEC cultures. **(A, B)** Cultures were monitored by phase-contrast microscopy at 72, 144, and 216 hours post treatment (hpt). **(A, B)** WT **(A)** WT and **(B)** Edmonston MV. **(C)** Immunofluorescence at 144 hpt for caspase 3 (red) and DAPI for nuclei (blue) in MBEC cultures treated with UV-inactivated S removed from WT MV and mock-infected cells at 96 hpi. Magnifications: **(A, B)** 200 $\times$ ; **(C)** 400 $\times$ .

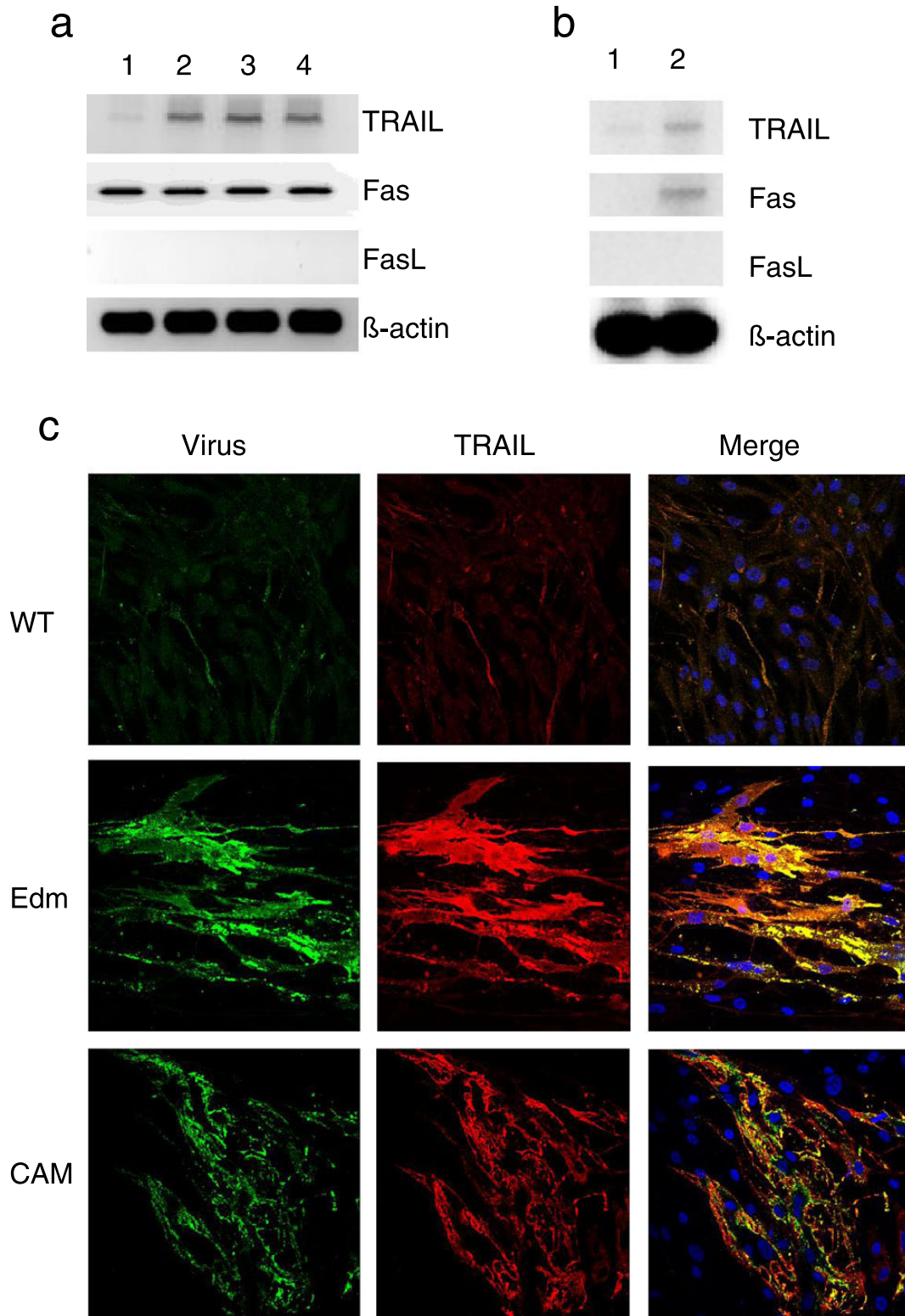


**FIGURE 6.** Soluble tumor necrosis factor–related apoptosis-inducing ligand (TRAIL) is induced by measles virus (MV) infection. Cultures were infected at a multiplicity of infection (MOI) of 5 with wild-type (WT) and Edmonston MV (human [HBECs] and murine [MBECs] brain endothelial cells) and CAM/RB (HBEC). RNA was prepared from WT MV-infected HBEC and MBEC monolayers; RT-PCR was carried out for Fas, Fas ligand (FasL), TRAIL, and  $\beta$ -actin mRNA. **(A)** MBEC: lane 1, mock infected; lane 2, WT MV 72 hpi; lane 3, WT MV 96 hpi; and lane 4, WT MV 120 hpi. **(B)** HBEC: Lane 1, mock infected; Lane 2 WT MV, 72 hpi. **(C)** Immunofluorescence was carried out on HBECs at 72 hpi for viral antigen (green), TRAIL (red), and nuclei (blue). Magnification: 200 $\times$ .

treated for 144 hours with supernatants removed from WT MV-infected and mock-infected cells at 96 hpi for caspase 3–positive cells. No caspase 3 staining was seen in mock- or isotype Ab control-treated monolayers, whereas a mean of  $13\% \pm 1.35\%$  of cells counted in 10 fields in each of 3 cultures was caspase 3–positive in infected cell supernatant-treated monolayers (Fig. 5C).

### Soluble TRAIL Induced by MV Infection Causes Apoptosis

To identify the factor(s) responsible for causing apoptosis, RNA was extracted from MBEC cultures mock infected or infected with the WT MV strain at 72, 96, and 120 hpi and in HBEC cultures at 72 hpi. Reverse transcription–PCR was carried out for Fas, FasL, and TRAIL. Fas mRNA was detected at similar levels in both infected and mock-infected cultures, whereas no FasL mRNA was detected in either case. Polymerase chain reaction products for TRAIL were obtained for all cultures, but only a weak band was observed for mock-infected cells (Fig. 6A, B).

To confirm that TRAIL was also induced by virus infection in HBEC, cultures were infected with the 3 MV strains for 72 hours and double stained for viral antigen and TRAIL. Wild-type MV again produced lower levels of antigen with no syncytia formation compared to the 2 vaccine-derived strains. TRAIL staining colocalized with viral antigen in all cases (Fig. 6C). TRAIL-positive cells were not observed in noninfected monolayers (not shown).

Ultraviolet-inactivated supernatants from mock-, WT-, and Edmonston MV-infected MBEC cultures were examined for soluble TRAIL from 2 to 5 dpi using an ELISA to determine whether the cells were excreting this factor. As expected, we detected higher expression of TRAIL in WT MV supernatants compared to the Edmonston or mock supernatants at all time points. In WT MV supernatants, TRAIL was significantly higher by 2 dpi than in mock-infected cultures and continued to rise to a mean of 1 ng/ml (equivalent to an optical density of 0.18) at 5 dpi. Significantly higher levels compared to mock-infected cells were only found at 5 dpi with Edmonston MV supernatants (Fig. 7A).

To confirm that TRAIL was inducing apoptosis, UV-inactivated supernatants isolated from WT MV-infected MBEC cultures at 96 hpi were untreated, treated with anti-TRAIL Ab (at different concentrations ranging from 5 to 20  $\mu\text{g/ml}$ ), or treated with 20  $\mu\text{g/ml}$  of an isotype nonimmune Ab before adding to fresh MBECs. Cells were incubated for 140 hours, and the monolayers were examined. Extensive cell rounding occurred in cultures exposed to untreated (Fig. 7B) or isotype Ab-treated (not shown) supernatants. Rounding was decreased in monolayers exposed to supernatants treated with 5 and 10  $\mu\text{g/ml}$  of Ab; treatment with 20  $\mu\text{g/ml}$  of anti-TRAIL resulted in monolayers comparable to control cultures with no supernatant treatment (Fig. 7B). Cells were stained for caspase 3, and the percentage of positive cells was assessed. Anti-TRAIL treatment of supernatants at the concentrations of 10 and 20  $\mu\text{g/ml}$  reduced the percentage of caspase 3–positive cells to a highly significant level compared to the untreated or isotype Ab-treated supernatants (Fig. 7C). To further confirm the role of TRAIL in apoptosis in MBECs, cells were treated

with different concentrations of soluble murine TRAIL ranging from 1 to 1,000 ng/ml for 24 hours. The percentage of caspase 3–positive cells in monolayers was very significantly higher compared to the mock-treated cells even at a concentration of TRAIL of 1 ng/ml where a mean of 8% of the cells were caspase positive (Fig. 7D). This observation agreed with the concentration of TRAIL found in supernatants from WT MV-infected cells at 5 dpi (Fig. 7B). The percentage of cell loss from each culture was also determined. This increased to 35% in cultures treated with 1,000 ng/ml compared to nontreated cultures (Fig. 7E).

### TRAIL Is Induced by MV Infection of the Murine CNS

To determine whether findings in vitro for TRAIL induction by MV reflected the situation in vivo, we infected groups of at least 3 mice intracerebrally with WT, Edmonston, and CAM/RB viruses for 4 days. Control animals were mock infected. CAM/RB-infected mice developed initial clinical signs of hyperactivity, followed by disorientation, awkward gait, and finally hind leg paralysis, and they become moribund by Day 4 or 5. Wild-type- and Edmonston MV-infected mice remained healthy. Immunoperoxidase staining for MV was carried to examine the location of virus infection and the morphology of infected cell types. In CAM/RB MV-infected brains, there was widespread staining in the cerebral cortex and hippocampus, as previously described (8, 21) (Fig. 8A, B). Most infected cells had a neuronal morphology. Noninfected inflammatory cells were seen infiltrating infected areas (Fig. 8A, B). In sections from WT (Fig. 8C, D) and Edmonston MV (not shown)-infected mice, there were many more isolated areas of infection with less inflammation. Cells with neuronal morphology were again the predominantly stained cell type. Infection of blood vessels was observed in both CAM/RB- and in WT MV-infected mice (Fig. 8A, C).

Brain sections were then double stained for cell-specific markers and virus and examined by confocal microscopy. This confirmed that infection occurred predominantly in neurons (Fig. 8E). In contrast, astrocyte infection was not observed (Fig. 8F). Despite extensive efforts using several different antibodies, we were unable to stain oligodendrocytes or microglia; however, we have previously shown using double staining that oligodendrocytes in ex vivo cultures from mice infected with all 3 MV strains are positive for viral antigen (8). Double staining for virus and CD34 demonstrated that ECs are infected in both WT- and CAM/RB MV-infected brains (Fig. 8G). Autofluorescing red blood cells were observed within the vessel lumen, but MV staining was demonstrated within the cytoplasm of cells in the vessel wall that also showed CD34 staining in their membranes.

Parallel sections were also double stained for MV and TRAIL (Fig. 9). TRAIL staining was observed predominantly in blood vessels with CAM/RB MV infection (Fig. 9A). Very few infected cells were observed in Edmonston vaccine strain-infected mice with associated low levels of TRAIL (Fig. 9B). Infection with WT virus resulted in focal areas of infection in the brain parenchyma. Many of these cells were double stained for TRAIL, but there were also virus-negative cells around the infected foci that were positive for

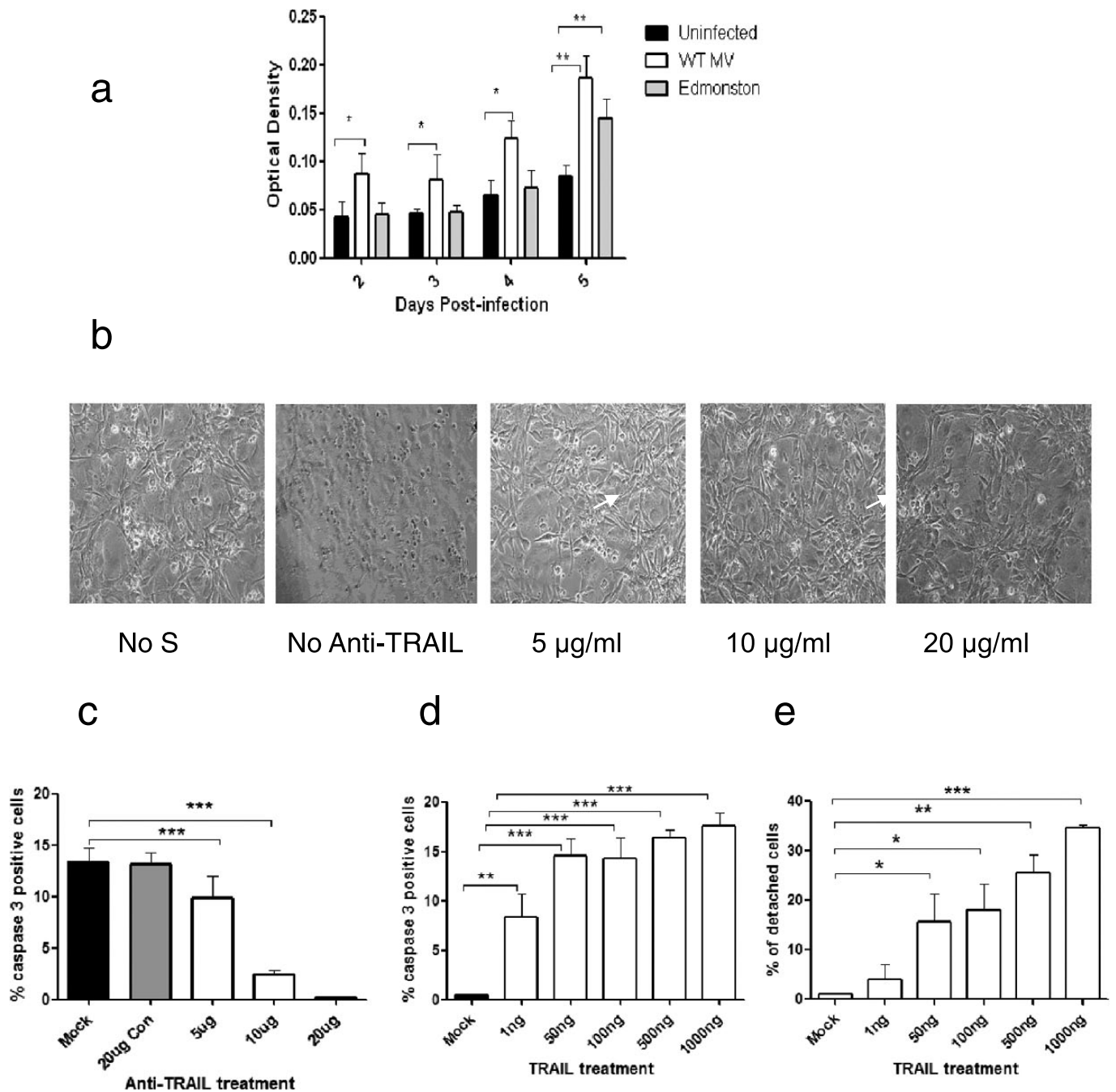


**FIGURE 7.** Tumor necrosis factor–related apoptosis-inducing ligand (TRAIL) induces apoptosis in brain endothelial cells (BEC). Murine BECs (MBECs) were infected at a multiplicity of infection (MOI) of 5 with wild-type (WT) or Edmonston measles virus (MV). Supernatants (S) were collected at 72 to 216 hours post infection (hpi) and UV-inactivated. **(A)** TRAIL in S was measured by sandwich ELISA. Mean and SD for 3 separate experiments are shown. **(B, C)** S aliquots removed at 96 hpi were untreated, treated with increasing concentrations of anti-TRAIL antibody (5, 10, and 20 µg/ml), or treated with 20 µg/ml of a nonimmune isotype before adding to fresh MBEC monolayers. **(B)** Cultures were incubated for 144 hpi and examined by phase-contrast microscopy (magnification: 200×) or **(C)** stained for activated caspase 3; 10 or more fields were counted, and the percentage of positive cells was determined. **(D, E)** MBECs were untreated or treated with increasing concentrations of soluble TRAIL (1, 50, 100, 500, and 1,000 ng/ml) for 24 hours. **(D)** Cells were stained for activated caspase 3; 10 or more fields were counted, and the percentage of positive cells was determined. **(E)** The percentages of cell loss relative to mock-treated cultures were determined. The mean and SD for 3 separate experiments are shown. \*,  $p < 0.05$ ; \*\*,  $p < 0.01$ ; \*\*\*,  $p < 0.001$ .

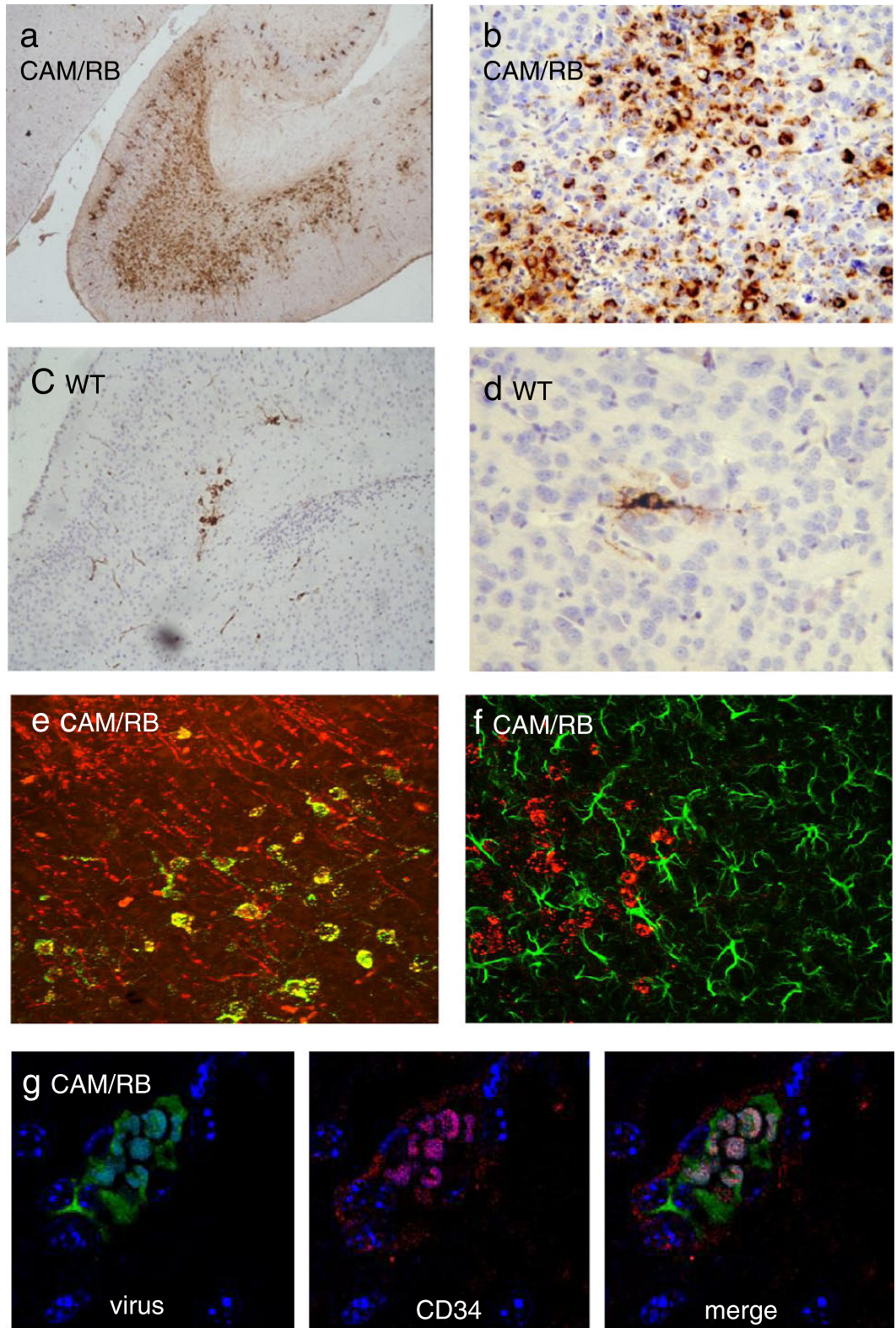


**FIGURE 8.** Measles virus (MV) antigen in neurons and endothelial cells in MV-infected mice. Two- to three-day-old mice were infected with  $10^4$  TCID<sub>50</sub> of CAM/RB or wild-type (WT) MV strains for 4 days. **(A–D)** Immunoperoxidase staining was carried out for MV; the sections were counterstained with hematoxylin. Brain sections from **(A,B)** CAM/RB MV -infected and **(C,D)** WT MV-infected mice are shown. **(E–G)** Double staining for MV and **(E)** MAP-2 for neurons (red), **(F)** GFAP for astrocytes (green), and **(G)** CD34 for endothelial cells (red). Magnifications: **(A, C)** 100×; **(B, DF)** 400×; **(G)** 630×.

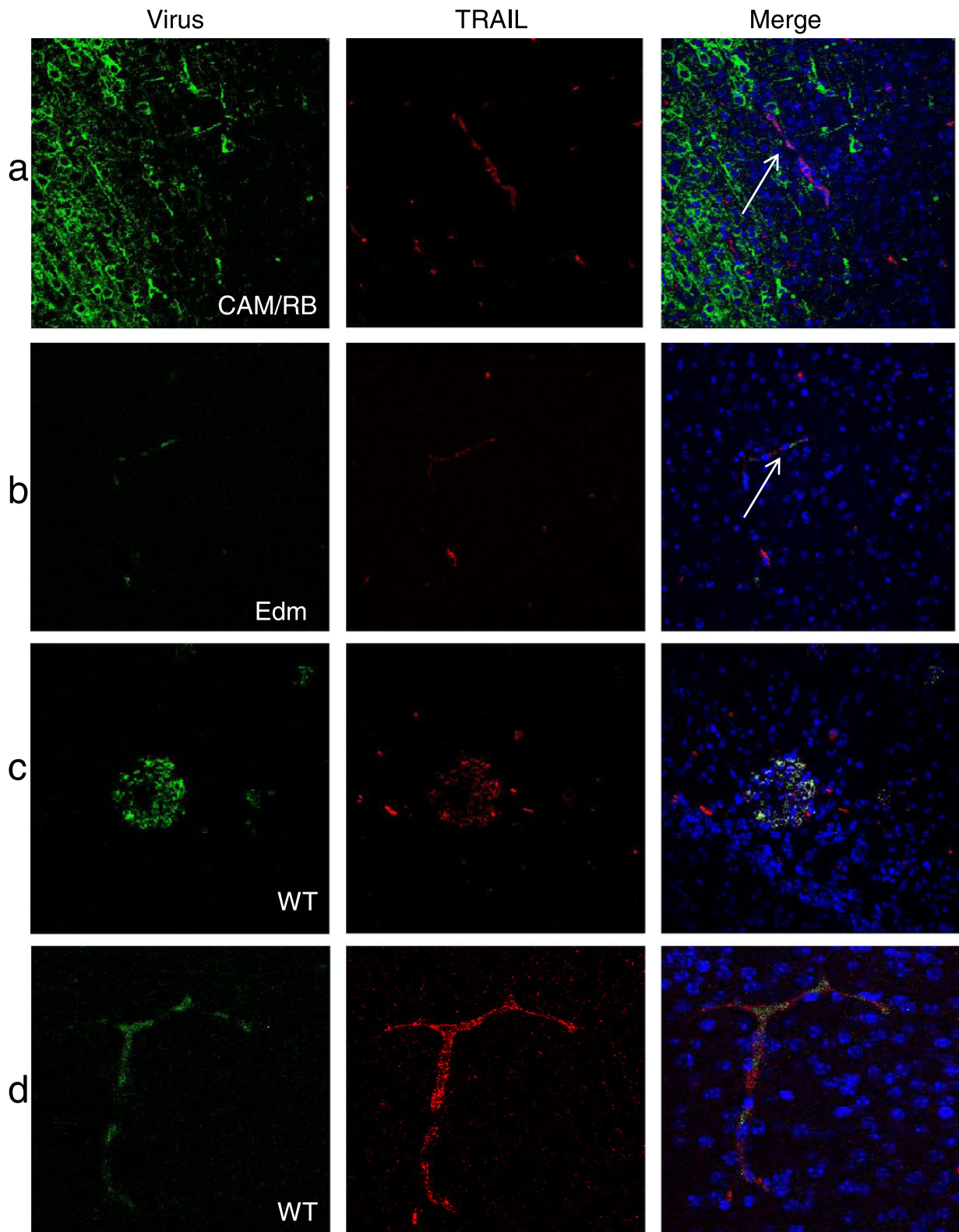


**FIGURE 9.** Tumor necrosis factor–related apoptosis-inducing ligand (TRAIL) is induced in murine cerebral endothelium by measles virus (MV) infection. Two- to three-day-old mice were infected with  $10^4$  TCID<sub>50</sub> of CAM/RB, Edmonston (Edm), or wild-type (WT) MV strains for 4 days. **(A–D)** Double immunofluorescent staining was carried out for MV and TRAIL. White arrows indicate blood vessels in **(A)** and **(B)**. A WT MV-infected focus and blood vessel showing WT MV antigen are shown in **(C)** and **(D)**, respectively. Magnifications: **(A–C)** 200×; **(D)** 400×.

TRAIL (Fig. 9C). For CAM/RB infection, TRAIL staining was also observed in blood vessels some of which were also positive for viral antigen (Fig. 9D). No TRAIL staining was observed in control brains (not shown).

## DISCUSSION

It has been postulated that parenchymal cells adjacent to infected ECs may occasionally become infected at the time of primary measles infection (2) and that this is the likely route of infection in individuals who develop MIBE and SSPE. Reports also suggest the important contribution of BECs to the process of spread of other viruses from the bloodstream to the surrounding tissues in the brain. These include HIV, Semliki Forest, West Nile, and human T-cell leukemia virus type 1 viruses (33–36).

Studies on HBEC have previously been carried out to examine infection with WT MV strains and transmigration of lymphocytes through ECs, but apoptotic mechanisms in these cells have not been addressed (7, 13). Furthermore, no suitable *in vivo* models of MV endothelial infection have previously been described. Therefore, we initially compared infection and apoptosis induced by WT, rodent-adapted, and vaccine strains of MV in HBEC and MBEC. The similarities observed, particularly with WT virus, validated subsequent *in vivo* infection of mice to model events at the BBB in SSPE and MIBE.

In MBECs, which do not express CD46, all viruses produced a low percentage of antigen-positive cells, as infection appeared to be restricted to a subpopulation of cells. Spread to other cells was possible when MBECs were overlaid with permissive Vero cells; this supports the view of lack of susceptibility of adjacent MBECs in the culture. Murine BECs are unlikely to be a homogeneous population because some cells in cultures have been shown to be more sensitive to radiation than others (37). It is possible that there are distinct phenotypes of BECs with each differing in permissiveness to infection. Alternatively, the cell cycle may affect virus replication because of the compartmental distribution at different stages.

In contrast to MBECs, up to 60% of HBECs were virus antigen positive for WT virus. These results are similar to those previously obtained for the W $\ddot{u}$ 4797 MV strain of MV that was shown to have relatively high levels both of binding to and infection of HBEC compared to other WT strains (13). However, both the W $\ddot{u}$ 4797 strain (13) and the Dublin 3267 strain used in the current study had lower levels of infection than vaccine-derived strains that can use CD46 as a receptor. It is possible that 1 or more receptors for WT MV are expressed on a higher percentage of HBECs than MBECs or that a different receptor is used in the latter. Surprisingly, in infected HBECs (but not MBECs) PVRL4 staining occurred in areas of virus infection, suggesting that the virus was upregulating this molecule in these cells. It has been observed that MV infection temporarily initially upregulates the virus receptor SLAM in monocytes and alveolar macrophages (15, 38, 39). Further studies will be necessary to determine whether PVRL4 is a receptor for MV in HBECs and if different WT virus strains can upregulate or use this molecule to different extents.

Extensive monolayer destruction was observed in infected cultures, most marked with WT MV. This suggested the production of 1 or more soluble factors that act on noninfected cells and was confirmed by treating fresh MBEC monolayers with UV infectivity-inactivated supernatants. Staining for activated caspase 3 in MBECs and HBECs was consistent with death by apoptosis. A recent study of a clinical isolate of dengue virus infection in human EC reported that apoptosis occurred through both caspase-dependent and -independent pathways (40). Similar to the studies of MV infection in dendritic cells (41–43), we could not detect FasL mRNA in uninfected cultures or induction after infection. Wosilk et al (44) reported that Fas (the FasL receptor) but not FasL was expressed on HBECs. We detected similar levels of Fas mRNA in both uninfected and infected MBECs and HBECs.

There is conflicting evidence as to whether TRAIL protects or causes apoptosis in peripheral ECs (45, 46). It has been shown recently that TRAIL death receptors DR4 and DR5 specifically mediate oligomeric amyloid  $\beta$  induction of extrinsic apoptotic pathways in HBECs with activation of both caspase 8 and caspase 9 (47). In the current study, we found that treatment of virally induced supernatants with anti-TRAIL Ab successfully blocked caspase 3 expression and MBEC destruction in a dose-dependent manner. TRAIL-specific antibodies have also been shown to inhibit apoptosis in human peripheral ECs treated with statins (48). Treatment of MBECs with murine TRAIL also confirmed the role of this factor in apoptosis. A recent study has shown that TRAIL mRNA is induced in HBECs by thrombospondin 1 (49), and we show that TRAIL protein expression is induced in both HBECs and MBECs after MV infection.

We have previously reported that apoptosis can be observed in both MV-infected human and murine brain (50) but did not specifically examine BEC. Mice only have 1 full-length TRAIL receptor, which has facilitated the production of knockout transgenics used in virus studies, but CNS infection has not been studied (51). We show that MV infection in the normal murine CNS is associated with TRAIL production, particularly in the endothelium, regardless of the level of parenchymal infection. TRAIL expression was detected in both infected and noninfected blood vessels in both CAM/RB- and WT MV-infected brains. Failure to detect virus in all TRAIL-positive ECs may relate to either the sensitivity of viral antigen detection or alternatively induction of TRAIL by soluble factors released from more distant infected cells.

In conclusion, our data are the first demonstration that infection of a low percentage of MBECs with WT MV allows efficient virus production as well as induction of TRAIL and subsequent widespread apoptosis. Whereas only a few infected BECs have been detected in SSPE brain tissue (5), these are likely to have a major effect on the disease process through both local virus production and virus-induced apoptosis. Endothelial cells have very low proliferation rates (52, 53), and therefore, small numbers of apoptotic cells would have a major effect with regard to breakdown of the BBB. Wild-type MV infection of BECs is likely to allow virus to invade the brain parenchyma in immunocompromised or other susceptible individuals with resultant bystander effects on neural cells. We have shown that WT MV infection



of MBEC appears to be very similar to that in HBEC and that infection of the endothelium and TRAIL production occurs in the murine CNS. These parallel in vitro and in vivo WT MV models can be used to develop therapeutic approaches, particularly for immunosuppressed individuals exposed to MV. This strategy may also be applicable to other virus infections.

**REFERENCES**

1. Perry RT, Halsey NA. The clinical significance of measles: A review. *J Infect Dis* 2004;189:S4–16.
2. Esolen LM, Takahashi K, Johnson RT, et al. Brain endothelial cell infection in children with acute fatal measles. *J Clin Invest* 1995; 96:2478–81
3. McQuaid S, Cosby SL, Koffi K, et al. Distribution of measles virus in the central nervous system of HIV-seropositive children. *Acta Neuropathol* 1998;96:637–42
4. Freeman AF, Jacobson DA, Shulman ST, et al. A new complication of stem cell transplantation: measles inclusion body encephalitis. *Pediatrics* 2004;114:e657–60
5. Kirk J, Zhou AL, McQuaid S, Cosby SL, et al. Cerebral endothelial cell infection by measles virus in subacute sclerosing panencephalitis: Ultrastructural and in situ hybridization evidence. *Neuropathol Appl Neurobiol* 1991;17:289–97
6. Rudd PA, Cattaneo R, von Messling V. Canine distemper virus uses both the anterograde and the hematogenous pathway for neuroinvasion. *J Virol* 2006;80:9361–70
7. Dittmar S, Harms H, Runkler N, et al. Measles virus–induced block of transendothelial migration of T lymphocytes and infection-mediated virus spread across endothelial cell barriers. *J Virol* 2008;82:11273–82
8. Abdullah H, Earle JA, Gardiner TA, et al. Persistent measles virus infection of mouse neural cells lacking known human entry receptors. *Neuropathol Appl Neurobiol* 2009;35:473–86
9. Brankin B, Hart MN, Cosby SL, et al. Adhesion molecule expression and lymphocyte adhesion to cerebral endothelium: Effects of measles virus and herpes simplex 1 virus. *J Neuroimmunol* 1995;5:1–8
10. Cosby SL, Brankin B. Measles virus infection of cerebral endothelial cells and effect on their adhesive properties. *Vet Microbiol* 1995; 44:135–39
11. McQuaid S, Cosby SL. An immunohistochemical study of the distribution of the measles virus receptors, CD46 and SLAM, in normal human tissues and subacute sclerosing panencephalitis. *Lab Invest* 2002; 82:403–9
12. Shusta EV, Zhu C, Boado RJ, et al. Subtractive expression cloning reveals high expression of CD46 at the blood-brain barrier. *J Neuropathol Exp Neurol* 2002;61:597–604
13. Andres O, Obojes K, Kim KS, et al. CD46- and CD150-independent endothelial cell infection with wild-type measles viruses. *J Gen Virol* 2003;84:1189–97
14. Cocks BG, Chang C-CJ, Carballido JM, et al. A novel receptor involved in T-cell activation. *Nature* 1995;376:260–63
15. Minagawa H, Tanaka N, Ono H, et al. Induction of measles virus receptor SLAM (CD150) on monocytes. *J Gen Virol* 2001;82:2913–17
16. Noyce RS, Bondre DG, Ha MN, et al. Tumor cell marker PVRL4 (nectin 4) is an epithelial cell receptor for measles virus. *PLoS Pathog* 2011;7:e1002240
17. Mühlebach MD, Mateo M, Sinn PL, et al. Adherens junction protein nectin-4 is the epithelial receptor for measles virus. *Nature* 2011; 480:530–33
18. Combredet C, Labrousse V, Mollet L, et al. A molecularly cloned Schwarz strain of measles virus vaccine induces strong immune responses in macaques and transgenic mice. *J Virol* 2003;77:11546–54
19. Liebert UG, ter Meulen V. Virological aspects of measles virus–induced encephalomyelitis in Lewis and BN rats. *J Gen Virol* 1987;68:1715–22
20. Coughlan S, Connell J, Cohen B, et al. Suboptimal measles-mumps-rubella vaccination coverage facilitates an imported measles outbreak in Ireland. *Clin Infect Dis* 2002;35:84–86
21. Galbraith SE, McQuaid S, Hamill L, et al. Rinderpest and peste des petits ruminants viruses exhibit neurovirulence in mice. *J Neurovirol* 2002;8:45–52

22. Zhang SX, Zhu C, Ba Y, et al. Gekko-sulfated glycopeptide inhibits tumor angiogenesis by targeting basic fibroblast growth factor. *J Biol Chem* 2012;287:13206–15
23. Hicks SD, Miller MW. Effects of ethanol on transforming growth factor B1-dependent and -independent mechanisms of neural stem cell apoptosis. *Exp Neurol* 2011;229:372–80
24. Li XX, Cheng C, Fei M, et al. Spatiotemporal expression of Dexas1 after spinal cord transection in rats. *Cell Mol Neurobiol* 2008;280:371–88
25. Sahay G, Gautam V, Luxenhofer R, et al. The utilization of pathogen-like cellular trafficking by single chain block copolymer. *Biomaterials* 2010; 31:1757–64
26. Hey F, Czyzewicz N, Jones P, et al. DEF6, a novel substrate for the Tec kinase ITK, contains a glutamine-rich aggregation-prone region and forms cytoplasmic granules that co-localize with P-bodies. *J Biol Chem* 2012;287:31073–84
27. Lentz SI, Edwards JL, Backus C, et al. Mitochondrial DNA (mtDNA) biogenesis: Visualization and dual incorporation of BrdU and EdU into newly synthesized mtDNA In Vitro. *J Histochem Cytochem* 2010; 58:207–18
28. Zhang P, Sridharan D, Lambert MW, et al. Knockdown of mu-calpain in Fanconi anemia, FA-A, cells by siRNA restores alphaII spectrin levels and corrects chromosomal instability and defective DNA interstrand cross-link repair. *Biochemistry* 2010;49:5570–81
29. Kim S, Jun DH, Kim HJ, et al. Development of a high-content screening method for chemicals modulating DNA damage response. *J Biomol Screen* 2011;16:259–65
30. Fleck M, Zhou T, Tatsuta T, et al. Fas/Fas ligand signalling during gestational T cell development. *J Immunol* 1998;160:3766–75
31. Fang Y, Sharp GC, Yagita H, et al. A critical role for TRAIL in resolution of granulomatous experimental autoimmune thyroiditis. *J Pathol* 2008; 216:505–13
32. Reymond N, Fabre S, Lecocq E, et al. Nectin4/PRR4, a new afadin-associated member of the nectin family that trans-interacts with nectin1/PRR1 through V domain interaction. *J Biol Chem* 2001;276: 43205–15
33. Nakaoka R, Ryerse JS, Niwa M, et al. Human immunodeficiency virus type 1 transport across the in vitro mouse brain endothelial cell monolayer. *Exp Neurol* 2005;193:101–9
34. Romero IA, Prevost MC, Perret E, et al. Interactions between brain endothelial cells and human T-cell leukemia virus type 1–infected lymphocytes: Mechanisms of viral entry into the central nervous system. *J Virol* 2000;74:6021–30
35. Soilu-Hänninen M, Erälänpää JP, Hukkanen V, et al. Semliki forest virus infects mouse brain endothelial cells and causes blood-brain barrier damage. *J Virol* 1994;68:6291–98
36. Verma S, Lo Y, Chapagain M, et al. West Nile virus infection modulates human brain microvascular endothelial cells tight junction proteins and cell adhesion molecules: Transmigration across the in vitro blood-brain barrier. *Virology* 2009;385:425–33
37. Lyubimova NV, Coultas PG, Yuen K, et al. In vivo radioprotection of mouse brain endothelial cells by Hoechst 33342. *Br J Radiol* 2001;74:77–82
38. Welstead GG, Hsu EC, Lorio C, et al. Mechanism of CD150 (SLAM) down regulation from the host cell surface by measles virus hemagglutinin protein. *J Virol* 2004;78:9666–74
39. Antunes Ferreira CS, Frenzke M, Leonard VHJ, et al. Measles virus infection of alveolar macrophages and dendritic cells precedes spread to lymphatic organs in transgenic mice expressing human signaling lymphocytic activation molecule (SLAM, CD150). *J Virol* 2010;84:3033–42.
40. Vasquez Ochoa M, Garcia Cordero J, Gutierrez Castaneda B, et al. A clinical isolate of dengue virus and its proteins induce apoptosis in HMEC-1 cells: A possible implication in pathogenesis. *Arch Virol* 2009; 154:919–28
41. Schneider-Schaulies S, Klagge IM, ter Meulen V. Dendritic cells and measles virus infection. *Curr Top Microbiol Immunol* 2003;276:77–101
42. Vidalain PO, Azocar O, Lamouille B, et al. Measles virus induces functional TRAIL production by human dendritic cells. *J Virol* 2005;74:556–59
43. Zilliox MJ, Parnigiani G, Griffin DE. Gene expression patterns in dendritic cells infected with measles virus compared with other pathogens. *Proc Natl Acad Sci U S A* 2006;103:3363–68
44. Wosik K, Cayrol R, Dodelet-Devillers A, et al. Angiotensin II controls occludin function and is required for blood brain barrier maintenance: relevance to multiple sclerosis. *J Neurosci* 2007;27:9032–42

45. Secchiero P, Gonelli A, Carnevale E, et al. TRAIL promotes the survival and proliferation of primary human vascular endothelial cells by activating the Akt and ERK pathways. *Circulation* 2003;107:2250–56
46. Alladina SJ, Song JH, Davidge ST, et al. TRAIL-induced apoptosis in human vascular endothelium is regulated by phosphatidylinositol 3-kinase/Akt through the short form of cellular FLIP and Bcl-2. *J Vasc Res* 2005;42:337–47
47. Fossati S, Ghiso J, Rostagno A. TRAIL death receptors DR4 and DR5 mediate cerebral microvascular endothelial cell apoptosis induced by oligomeric Alzheimer's A $\beta$ . *Cell Death Dis* 2012;3:e321
48. Sato K, Nuki T, Gomita K, et al. Statins reduce endothelial cell apoptosis via inhibition of TRAIL expression on activated CD4 T cells in acute coronary syndrome. *Atherosclerosis* 2010;213:33–39
49. Rege TA, Stewart J Jr, Dranka B, et al. Thrombospondin-1-induced apoptosis of brain microvascular endothelial cells can be mediated by TNF-R1. *J Cell Physiol* 2009;218:94–103
50. McQuaid S, McMahon J, Herron B, et al. Apoptosis in measles virus-infected human central nervous system tissues. *Neuropathol Appl Neurobiol* 1997;23:218–24
51. Cummins N, Badley A. The TRAIL to viral pathogenesis: The good, the bad and the ugly. *Curr Mol Med* 2009;9:495–505
52. Hobson B, Denekamp J. Endothelial proliferation in tumours and normal tissues: Continuous labelling studies. *Br J Cancer* 1984;49:405–13
53. Korr H, Schultze B, Maurer W. Autoradiographic investigations of glial proliferation in the brain of adult mice. II. Cycle time and mode of proliferation of neuroglia and endothelial cells. *J Comp Neurol* 1975;160:477–90